1
Elementary quantum electrodynamical processes in multimode scenarios - a photon path representation for multiphoton states

Nils Trautmann and Gernot Alber

The field of quantum optics has experienced remarkable experimental developments during the last decades [1, 2, 3]. Progress in controlling single quantum emitters, such as trapped atoms or ions, and the ability to tailor the mode structure of the electromagnetic radiation field by using high finesse cavities has enabled new possibilities in studying resonant light-matter interactions. This led to a variety of of remarkable experiments [4, 5, 6] probing the interaction between single quantum emitters and selected modes of the radiation field and demonstrating quantum communication and quantum information processing [7, 8, 9, 10, 11]. However, the implementation of quantum networks based on high finesse cavities coupled to suitable waveguides is still challenging due to lossy connections between cavities and waveguides.

A new approach for harnessing the nonlinear interaction between light and single quantum emitters is to enhance matter field couplings in the absence of a strongly mode selective optical resonator by confining the photons to sub wavelength length scales. This can be achieved by suitable one-dimensional waveguides, such as nanowires [12, 13, 14, 15, 16], nanofibers [17, 18], in coplanar waveguides (circuit QED) [19, 20], or even in free space [21] by focusing the light using a parabolic mirror. However, these approaches are inherently connected to multimode scenarios in which a large number of field modes participates in the coupling of the quantum emitters to the radiation field. This vast number of degrees of freedom complicates the theoretical investigation especially if highly non-classical multiphoton states, such as photon number states, are involved in the systems dynamics. Such states have already been realized in experiment [22, 23, 24] and are of significant interest for applications in quantum information processing and quantum communication. Hence, there is a need for developing suitable theoretical methods to treat such matter field interactions involving highly non-classical multiphoton states in multimode scenarios.

In recent years several methods addressing this issue have been developed. The Bethe-ansatz [25] as well as the the input output formalism [26] have been used to analyze photon transport in waveguides with an embedded qubit and one and two-photon scattering matrix elements have been evaluated [27, 28]. With similar techniques also scattering matrix elements for even higher photon number states have

been evaluated [29, 30, 31, 32]. Recently, the input-output formalism has been generalized to treat many spatially distributed atoms coupled to a common waveguide [33]. Particular interesting phenomena arise if non Markovian processes are investigated. Recently, a multiphoton scattering theory has been developed to treat [34] these kind of situations and has been used to evaluate the scattering matrix elements for several scenarios of interest. Starting from initially prepared coherent states and analogously to the technique developed by Mollow [35] displacement transformations are applied and generalized master equations have been derived for describing the dynamics.

In this chapter we focus on this line of research and discuss a systematic diagrammatic method for evaluating the time evolution of highly non-classical multiphoton number states interacting with multiple quantum emitters in multimode scenarios. It allows the interpretation of the system's dynamics in terms of sequences of spontaneous photon emission and absorption processes interconnected by photon propagation between quantum emitters or involving reflection by the boundary of a waveguide or a mirror. This photon path representation for multiphoton states allows us not only to evaluate transition amplitudes between initial and final states in form of a scattering matrix but also enables us to study the full time evolution of the quantum state describing the closed system consisting of emitters, of the radiation field, and of possible boundary surfaces. This photon path representation is not only restricted to the description of one-dimensional waveguides but can also be used to evaluate the time evolution of several quantum emitters interacting with the radiation field in large or half-open cavities or even in free space. For the sake of simplicity, however, we restrict our subsequent considerations to two-level systems. But it is straight forward to generalize this multiphoton path representation also to more general multilevel systems.

A major advantage of this photon path representation for multiphoton states is that only a finite number of diagrams has to be taken into account for determining the time evolution of finitely many photons over a finite time interval. This is achieved by exploiting the retardation effects caused by the multimode radiation field and basic properties of initially prepared photon number states. The accuracy of this diagrammatic method is only limited by the typical quantum optical approximations, namely the dipole approximation and the assumption that the timescale induced by the atomic transition frequencies is by far the shortest one. Thus, this method offers a systematic possibility to study non linear and non Markovian processes induced by resonant matter-field interactions involving highly non-classical multiphoton states and the full multimode description of the radiation field. This is not only interesting from an applied perspective in order to accomplish tasks relevant for quantum information processing, for example, but also from a fundamental point of view.

This chapter is organized as follows. In Sec. 1.1 we introduce a generic theoretical model and discuss the main approximations. The multiphoton path representation for describing the time evolution of relevant quantum mechanical transition amplitudes is presented in Sec. 1.2 and is applied to physical scenarios in Sec. 1.3 .

1.1
A generic quantum electrodynamical model

We investigate the dynamics of N quantum emitters, e.g. atoms or ions, situated at the positions $\mathbf{x}_A$ ($A \in \{1, 2, ...N\}$) interacting almost resonantly with the radiation field in a large or half-open cavity or in free space. For the sake of simplicity we assume that the quantum emitters can be modelled by identical two-level atoms or qubits whose center of mass motion is negligible. The dipole matrix element of atom A is denoted by $\mathbf{d}_A = \langle e|_A \hat{\mathbf{d}}_A |g\rangle_A$ and the corresponding transition frequency is ω_{eg}. In the following we assume that the dipole and the rotating-wave approximation (RWA) are applicable. For justifying the RWA we assume that the timescale induced by the atomic transition frequency ω_{eg} is by far the shortest one. The interaction between the two-level atoms and the quantized (transverse) electromagnetic radiation field is described by the Hamiltonian

$$\hat{H} = \hat{H}_0 + \hat{H}_1 \tag{1.1}$$

with

$$\begin{aligned} \hat{H}_0 &= \sum_i \hbar\omega_i \hat{a}_i^\dagger \hat{a}_i + \hbar\omega_{\mathrm{eg}} \sum_{A=1}^{N} |e\rangle_A \langle e|_A \ , \\ \hat{H}_1 &= -\sum_{A=1}^{N} \hat{\mathbf{E}}_\perp^-(\mathbf{x}_A) \cdot \hat{\mathbf{d}}_A^- + \mathrm{H.c.} \end{aligned} \tag{1.2}$$

and with the dipole transition operator

$$\hat{\mathbf{d}}_A^- = \left(\hat{\mathbf{d}}_A^+\right)^\dagger = \mathbf{d}_A^* |g\rangle_A \langle e|_A \tag{1.3}$$

of atom A. The coupling to the radiation field is modeled by introducing the electric field operators $\hat{\mathbf{E}}_\perp^\pm(\mathbf{x}_A)$ of the transverse modes of the radiation field. In the Schrödinger picture they are given by

$$\hat{\mathbf{E}}_\perp^-(\mathbf{x}) = \left(\hat{\mathbf{E}}_\perp^+(\mathbf{x})\right)^\dagger = -\mathrm{i}\sum_i \sqrt{\frac{\hbar\omega_i}{2\epsilon_0}} \mathbf{g}_i(\mathbf{x}) \hat{a}_i^\dagger \tag{1.4}$$

with the orthonormal mode functions $\mathbf{g}_i(\mathbf{x})$. The mode function $\mathbf{g}_i(\mathbf{x})$ solves the Helmholtz equation and fulfills the boundary conditions modelling the presence of a possible cavity or of a wave guide.

1.2
The multiphoton path representation

A solution of the time dependent Schrödinger equation of the generic quantum electrodynamical model with Hamiltonian (1.1) can be obtained conveniently with the help of a photon path representation.

1.2.1 Analytical solution of the Schrödinger equation

Let us consider the time evolution of an initially prepared quantum state with n_P photonic and n_A atomic excitations, i.e.

$$|\psi(t_0)\rangle = \prod_{i=1}^{n_P} \left(\sum_j f_j^{(i)}(t_0) a_j^\dagger \right) |0\rangle^P \prod_{k=1}^{n_A} |e\rangle_{A_k} \langle g|_{A_k} |G\rangle^A , \tag{1.5}$$

with $|0\rangle^P$ denoting the vacuum state of the radiation field and with $|G\rangle^A = |g\rangle_1 \ldots |g\rangle_N$ denoting the ground state of all two-level atoms. Each of the sums $\sum_j f_j^{(i)}(t_0) a_j^\dagger$ represents a single photon wave packet and the amplitudes $f_j^{(i)}(t_0)$ fulfill the normalization condition $\langle \psi(t_0), \psi(t_0) \rangle = 1$.

The Schrödinger equation with Hamiltonian (1.1) fulfilling this initial condition is equivalent to an integral equation whose solution can be obtained with the help of a fix-point iteration procedure. In the interaction picture with Hamiltonian $\hat{\tilde{H}}_1(t) = e^{\mathrm{i}/\hbar \hat{H}_0 (t-t_0)} \hat{H}_1 e^{-\mathrm{i}/\hbar \hat{H}_0 (t-t_0)}$ and quantum state $|\tilde{\psi}(t)\rangle$ this Schrödinger equation and its associated integral equation are given by

$$\mathrm{i}\hbar \frac{d}{dt} |\tilde{\psi}(t)\rangle = \hat{\tilde{H}}_1(t) |\tilde{\psi}\rangle \, , |\tilde{\psi}(t)\rangle = -\frac{\mathrm{i}}{\hbar} \int_{t_0}^{t} \hat{\tilde{H}}_1(t_1) |\tilde{\psi}(t_1)\rangle \, dt_1 + |\psi(t_0)\rangle \ . \tag{1.6}$$

In order to develop an iteration procedure for solving this equation which terminates after a finite number of iterations for any given finite time interval of duration $t - t_0$ it is necessary to take into account directly all processes describing spontaneous photon emission and reabsorption before a photon has had time to leave the atom. These processes take place during a time interval of the order of $1/\omega_{eg}$ and are responsible for spontaneous decay of an excited atom and for a small level shift of its transition frequency ω_{eg} [35, 36]. It turns out that all the other possible photon emission and absorption processes are delayed by retardation effects caused by photon propagation and characterized by the finite speed of light in vacuum c_0. These retardation effects cause the corresponding iteration procedure to terminate after a finite number of iterations in any finite interval or for a finite number of initially prepared photons.

For this iteration procedure the solution of the integral equation (1.6) is split into two parts according to

$$|\tilde{\psi}(t)\rangle = -\tfrac{\mathrm{i}}{\hbar} \textstyle\int_{t-\epsilon}^{t} \hat{\tilde{H}}_1(t_1) |\tilde{\psi}(t_1)\rangle \, dt_1 - \tfrac{\mathrm{i}}{\hbar} \int_{t_0}^{t-\epsilon} \hat{\tilde{H}}_1(t_1) |\tilde{\psi}(t_1)\rangle \, dt_1 + |\psi(t_0)\rangle \tag{1.7}$$

with $\epsilon \omega_{eg} \gg 1$. Inserting Eq. (1.7) into the Schrödinger equation (1.6) yields

$$\mathrm{i}\hbar \tfrac{d}{dt} |\tilde{\psi}(t)\rangle = \hat{\tilde{H}}_1(t) |\tilde{\psi}(t-\epsilon)\rangle - \tfrac{\mathrm{i}}{\hbar} \textstyle\int_{t-\epsilon}^{t} \hat{\tilde{H}}_1(t) \hat{\tilde{H}}_1(t_1) |\tilde{\psi}(t_1)\rangle \, dt_1 \ . \tag{1.8}$$

By applying the definition of $\hat{\tilde{H}}_1(t_1)$ we get

$$\hat{\tilde{H}}_1(t_2) \hat{\tilde{H}}_1(t_1) =: \hat{\tilde{H}}_1(t_2) \hat{\tilde{H}}_1(t_1) : + \sum_{A_1, A_2} |e\rangle_{A_2} \langle g|_{A_2} |g\rangle_{A_1} \langle e|_{A_1}$$
$$e^{\mathrm{i}\omega_{eg}(t_2 - t_1)} \left[\hat{\mathbf{E}}_\perp^+(\mathbf{x}_{A_2}, t_2) \cdot \mathbf{d}_{A_2}, \hat{\mathbf{E}}_\perp^-(\mathbf{x}_{A_1}, t_1) \cdot \mathbf{d}_{A_1}^* \right] \tag{1.9}$$

with $\hat{\mathbf{E}}_\perp^\pm(\mathbf{x}_a, t)$ denoting the electric field operators in the interaction picture and with $: \ldots :$ denoting normal ordering. The commutator in the last term of Eq. (1.9)

can be associated with the propagation of a photon emitted by atom A_1 to atom A_2 where it is absorbed again. As outlined in the Appendix for photon propagating in vacuum this commutator can be related to a dyadic Green operator of the d'Alembert equation. As the dispersion relation of the radiation field is linear this commutator can be evaluated in a straight forward way yielding the result

$$e^{\mathrm{i}\omega_{eg}(t_2-t_1)}\left[\hat{\mathbf{E}}_\perp^+(\mathbf{x}_{A_2},t_2)\cdot\mathbf{d}_{A_2},\hat{\mathbf{E}}_\perp^-(\mathbf{x}_{A_1},t_1)\cdot\mathbf{d}_{A_1}^*\right]=\delta_{A_1,A_2}\hbar^2\Gamma\delta(t_1-t_2) \quad (1.10)$$

for all $|t_1-t_2|<\tau_{A_1,A_2}$ and $\Gamma=||\mathbf{d}_{A_2}||^2\omega_{eg}^3/(3c_0^3\pi\epsilon_0\hbar)$ being the spontaneous decay rate of an atom in free space with the dielectric constant of the vacuum ϵ_0. The constant $\tau_{A_1,A_2}>0$ is the time a photon emitted by atom A_1 needs to propagate to atom A_2. In the special case $A_1=A_2$ it is the time a photon emitted by A_1 needs to return againto the same atom after being reflected by the boundary of a waveguide or by the surface of a cavity. In free space such a recurrence is impossible, i.e. $\tau_{A_1,A_1}=\infty$. The delta distribution appearing in Eq. (1.10) originates from the rotating wave approximation in which physical processes taking place during time scales of the order of $1/\omega_{eg}$ are approximated by instantaneous processes [35]. Thus, Eq. (1.10) reflects the fact that spontaneous emission and reabsorption of a photon before it has left the atom again requires a time scale of the order of $1/\omega_{eg}$ and is responsible for the spontaneous decay of an atom in free space. Furthermore, Eq. (1.10) assumes that the small shift of the transition frequency (Lamb-shift) has already been incorporated in a properly renormalized atomic transition frequency ω_{eg}.

Using Eq. (1.10) and choosing $0<\epsilon<\tau_{A_1,A_2}$ for all A_1,A_2 the Schrödinger equation (1.6) simplifies to

$$\begin{aligned}\frac{d}{dt}|\widetilde{\psi}(t)\rangle &= -\hat{\Gamma}/2\,|\widetilde{\psi}(t)\rangle-\frac{\mathrm{i}}{\hbar}\hat{\tilde{H}}_1(t)\,|\widetilde{\psi}(t-\epsilon)\rangle\\ &\quad-\frac{1}{\hbar^2}\int_{t-\epsilon}^{t}:\hat{\tilde{H}}_1(t)\hat{\tilde{H}}_1(t_1):|\widetilde{\psi}(t_1)\rangle\,dt_1\end{aligned} \quad (1.11)$$

with $\hat{\Gamma}=\Gamma\sum_{A=1}^{N}|e\rangle_A\langle e|_A$. Together with the initial condition (1.5) Eq. (1.11) is equivalent to the integral equation

$$\begin{aligned}|\widetilde{\psi}(t)\rangle &= e^{-\hat{\Gamma}(t-t_0)/2}\,|\psi(t_0)\rangle-\frac{\mathrm{i}}{\hbar}\int_{t_0}^{t}e^{-\hat{\Gamma}(t-t_1)/2}\hat{\tilde{H}}_1(t_1)\,|\widetilde{\psi}(t_1-\epsilon)\rangle\,dt_1\\ &\quad-\frac{1}{\hbar^2}\int_{t_0}^{t}\int_{t_2-\epsilon}^{t_2}e^{-\hat{\Gamma}(t-t_2)/2}:\hat{\tilde{H}}_1(t_2)\hat{\tilde{H}}_1(t_1):|\widetilde{\psi}(t_1)\rangle\,dt_1dt_2\end{aligned} \quad (1.12)$$

which can be solved by using a fix point iteration starting with $|\widetilde{\psi}(t)\rangle=0$. In the limit $\epsilon\to0$ in the physical sense of $1/\omega_{eg}\ll\epsilon\ll1/\Gamma$ its solution is given by the multiphoton path representation

$$\begin{aligned}|\widetilde{\psi}(t)\rangle&=\sum_{m=0}^{\infty}\left(-\tfrac{\mathrm{i}}{\hbar}\right)^m\lim_{\epsilon\to0}\int_{t_0}^{t}\int_{t_0}^{t_m-\epsilon}\ldots\int_{t_0}^{t_3-\epsilon}\int_{t_0}^{t_2-\epsilon}e^{-\hat{\Gamma}(t-t_m)/2}\\ &\mathcal{T}\left[\prod_{l=1}^{m}\hat{\tilde{H}}_1(t_l)e^{-\hat{\Gamma}(t_l-t_{l-1}-\epsilon)/2}\right]|\psi(t_0)\rangle\,dt_1dt_2\ldots dt_{m-1}dt_m\end{aligned} \quad (1.13)$$

with $\mathcal{T}$ denoting the time ordering operator. In this solution it has been taken into account that the contributions from the last line of Eq. (1.12) vanish in the physically

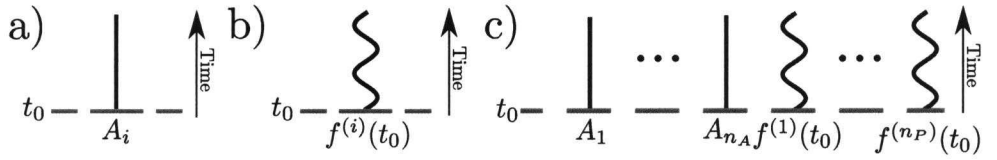

Figure 1.1 Diagrammatic representation of the excitations contributing to the initial state $|\psi(t_0)\rangle$ of Eq. (1.5): representation of (a) an initial atomic excitation, (b) an initial photonic excitation and (c) the initial state $|\psi(t_0)\rangle$.

relevant limit $\epsilon \to 0$. The sum of normally ordered terms appearing in Eq. (1.13) can be evaluated by introducing the functions

$$T_1^{A_1,A_2}(t_2-t_1) = \frac{1}{\hbar^2} e^{\mathrm{i}\omega_{eg}(t_2-t_1)} \left[\hat{\mathbf{E}}_\perp^+(\mathbf{x}_{A_2},t_2)\cdot\mathbf{d}_{A_2}, \hat{\mathbf{E}}_\perp^-(\mathbf{x}_{A_1},t_1)\cdot\mathbf{d}_{A_1}^*\right] - \delta_{A_2,A_1}\Gamma\delta(t_2-t_1). \tag{1.14}$$

They describe the retardation effects arising from spontaneous photon emission and reabsorption processes. Thus, only finitely many terms contribute to the sum of Eq. (1.12), if a finite time interval and an initial photon state with a finite number of photons are considered.

1.2.2 Graphical representation of the multiphoton path representation

For applying the previously derived multiphoton path representation of Eq. (1.13) and for giving a physical interpretation in terms of subsequent photon emission and absorption processes a diagrammatic method can be developed. Thereby, each term generated by applying Eq. (1.14) in order to bring Eq. (1.13) into a normally ordered form is represented graphically by a diagram. By generating the finite number of all possible diagrams and summing up their contributions allows to determine the time evolution of the quantum state $|\widetilde{\psi}(t)\rangle$ for any finite time. In the following we list the basic elements constituting such a diagram, provide a list of rules for generating all possible diagrams, and discuss the connection between these diagrams and the corresponding analytical expressions in the multiphoton path representation of Eq. (1.13).

Let us start with the graphical representation of the initial state $|\psi(t_0)\rangle$ of Eq. (1.5). An initial atomic excitation of an atom A_i is represented by a graphical element of the form depicted in Fig. 1.1 (a) and an initial photonic excitation corresponding to a term $\sum_j f_j^{(i)}(t_0)a_j^\dagger$ is represented by an element of the form depicted in Fig. 1.1 (b). Correspondingly, the initial state defined in Eq. (1.5) is represented by the diagram depicted in Fig. 1.1 (c).

We can also represent the excitations contributing to the state $|\widetilde{\psi}(t)\rangle$ of Eq. (1.13) in a similar way. Thereby, each atomic excitation of the state $|\widetilde{\psi}(t)\rangle$ is represented by a graphical element of the form depicted in Fig. 1.2 (a) and denotes an outgoing atomic excitation. Each photonic excitation of the state $|\widetilde{\psi}(t)\rangle$ is represented by an element of the form depicted in Fig. 1.2 (b) and denotes an outgoing photonic exci-

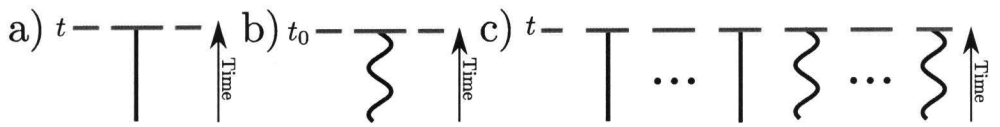

Figure 1.2 Diagrammatic representation of the excitations contributing to the state $|\widetilde{\psi}(t)\rangle$ of Eq. (1.13): representation of (a) an outgoing atomic excitation, (b) an outgoing photonic excitation and (c) the excitations of the state $|\widetilde{\psi}(t)\rangle$.

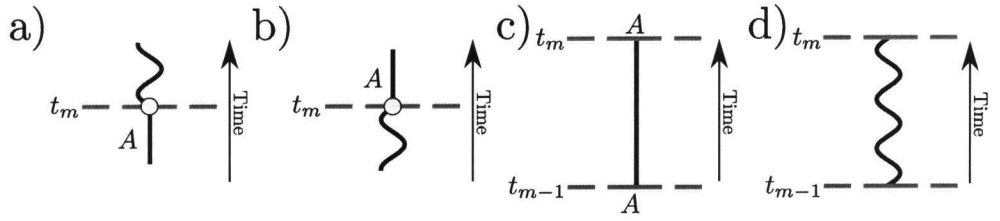

Figure 1.3 Diagrammatic representation of basic processes: representation of (a) an emission of a photon by an excited atom, (b) an absorption of a photon by an atom in the ground state, (c) propagation of an atomic excitation (atomic excitation line) and (d) propagation of a photonic excitation (photonic excitation line).

tation. Correspondingly, the state $|\widetilde{\psi}(t)\rangle$ is represented by the diagram of Fig. 1.2 (c).

Photon emission and absorption processes involving an atom A at the intermediate time step t_m (with $t > t_m > t_0$), are represented by the diagrams of 1.3 (a) and 1.3 (b). The propagation of atomic or photonic excitations during these processes are represented by the diagrams depicted in Figs. 1.3 (c) and Fig. 1.3 (d). These atomic and photonic excitation lines connect emission processes, absorption processes, and initial and outgoing excitations. In a diagram, an atomic excitation line refers to a single atom only, i.e. its beginning and its end connect the same atom.

These graphical elements are assembled to a complete diagram according to a set of rules. For a process involving m absorption and emission processes taking place at intermediate time steps $t_1 ... t_m$ with $t_0 < t_1 < t_2 < ... < t_m < t$ these rules are as follows:

1) At each emission process exactly one photon line starts and exactly one atomic excitation line ends.
2) At each absorption process exactly one atomic excitation line starts and exactly one photon line ends.
3) Each atomic excitation line starts either at an initial atomic excitation or at an absorption process and it ends either at an outgoing atomic excitation or at an emission process.
4) Each photon line starts either at an initial photonic excitation or at an emission process and it ends either at an outgoing photonic excitation or at an absorption process.
5) Atomic excitation lines corresponding to the same atom cannot coexist.

In particular, the last rule encodes effects originating from the saturation of an atomic

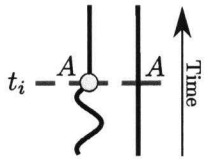

Figure 1.4 A forbidden diagram: The diagram describes a process in which an already excited atom A absorbs a photon. By excluding such diagrams all saturation effects are taken into account which characterize the excitation of two-level atoms.

transition. Thus, diagrams containing parts, such as the one depicted in Fig. 1.4 are forbidden. Ignoring this latter rule would result in a time evolution in which atoms would behave similarly as harmonic oscillators which do not show any saturation effects.

The rules connecting each diagram of this graphical representation with a corresponding term of the multiphoton path representation of $|\tilde{\psi}(t)\rangle$ of Eq. (1.13)) are as follows:

1) To a photon line connecting an emission process of atom A_e at time t_e with an absorption process at time t_a ($t_a > t_e$) by atom A_a we associate the term $-T_1^{A_e,A_a}(t_a - t_e)$.
2) To a photon line connecting an initial photonic excitation $f^{(i)}(t_0)$ with an absorption process at atom A_a and time t_a we associate a term $\frac{\mathrm{i}}{\hbar}\left[\hat{\mathbf{E}}_\perp^+(\mathbf{x}_{A_a}, t_a)\cdot\mathbf{d}_{A_a}, \sum_j f_j^{(i)}(t_0)a_j^\dagger\right] e^{\mathrm{i}\omega_{eg}(t_a-t_0)}$.
3) To a photon line connecting an initial photonic excitation $f^{(i)}(t_0)$ with an outgoing photonic excitation we associate a term $\sum_j f_j^{(i)}(t_0)a_j^\dagger$.
4) To a photon line connecting an emission process of atom A_e at time t_e with an outgoing photonic excitation we associate a term $\frac{\mathrm{i}}{\hbar}\hat{\mathbf{E}}_\perp^-(\mathbf{x}_{A_e}, t_e)\cdot\mathbf{d}_{A_e}^* e^{-\mathrm{i}\omega_{eg}(t_e-t_0)}$.
5) To an atomic excitation line not ending at an outgoing atomic excitation and starting and ending at times t_b and t_e we associate a term $e^{-\Gamma(t_e-t_b)/2}$.
6) To an an outgoing atomic excitation and starting at time t_b we associate a term $e^{-\Gamma(t-t_b)/2}\,|e\rangle_A\,\langle g|_A$.

The expression assigned to a complete diagram is given by the product of all these terms acting on the state $|G\rangle^A\,|0\rangle^P$ and being integrated over all intermediate time steps $t_1, t_2 ... t_m$ with $t_0 < t_1 < t_2 < ... < t_m < t$. The quantum state at time t, i.e. $|\tilde{\psi}(t)\rangle$, is obtained by summing over all possible equivalence classes of diagrams which can be constructed by these rules. Thereby, each equivalence class of diagrams appears in this sum only once. Two diagrams are considered to be equivalent if the corresponding photon and atomic excitation lines connect emission and absorption processes which involve the same atoms at the same time steps $t_1 ... t_n$ and the same initial and final excitations.

So far, we have restricted our discussion to identical two level systems. However, it is straight forward to generalize this multiphoton path representation also to multilevel atoms by following the steps of the previous subsection 1.2.1. This way an

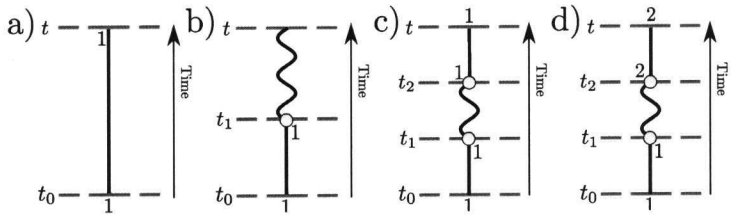

Figure 1.5 (a)-(c): Diagrammatic representation of the spontaneous photon emission of a single atom (atom 1) in free space or in an open waveguide. (d): Diagram describing a transfer of the excitation from the initially excited atom 1 to atom 2 mediated by a single photon.

expression quite similar to Eq. (1.13) can be derived and can be represented by an analogous diagrammatic procedure.

1.3 Examples

1.3.1 Processes involving only a single excitation

In order to discuss basic features of the multi-photon path representation and of the corresponding diagrammatic representation let us consider the simplest quantum electrodynamical processes involving a single excitation only. This way a direct connection can be established between this multiphoton path representation and photon path representations which have been discussed in the literature previously in connection with single photon processes [37, 38, 39].

Let us consider the spontaneous decay of a single initially excited atom coupled to the radiation field in free space or in an open waveguide. In free space this process is described by the diagrams depicted in Figs. 1.5 (a) and 1.5 (b). According to the rules of the previous section the diagram depicted in Fig. 1.5 (a) is associated with the contribution

$$e^{-\Gamma(t-t_0)/2}\,|e\rangle_1\,|0\rangle^P \tag{1.15}$$

to Eq. (1.13). It describes the decay of the excited atomic state due to the spontaneous emission of a photon. The emitted single-photon wave packet is described by the contribution to Eq. (1.13) associated with the diagram of Fig. 1.5 (b), i.e.

$$\frac{\mathrm{i}}{\hbar}\,|g\rangle_1 \int_{t_0}^{t} \hat{\mathbf{E}}_\perp^-(\mathbf{x}_1,t_1)\cdot\mathbf{d}_1^*\,|0\rangle^P\, e^{-(\Gamma/2+\mathrm{i}\omega_{eg})(t_1-t_0)}dt_1\ . \tag{1.16}$$

The diagram of next higher order is depicted in Fig. 1.5 (c) and corresponds to the term

$$-\,|e\rangle_1\,|0\rangle^P \int_{t_0}^{t}\int_{t_0}^{t_2} e^{-\Gamma(t-t_2)/2}T_1^{1,1}(t_2-t_1)e^{-\Gamma(t_1-t_0)/2}dt_1dt_2 \tag{1.17}$$

with $T_1^{1,1}(t_2-t_1)$ describing the return and reabsorption of a photon by atom 1 after having being emitted by the same atom. In general, such a process gives

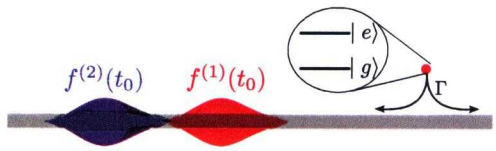

Figure 1.6 A schematic setup: Two photons with initial states $f^{(1)}(t_0)$ and $f^{(2)}(t_0)$ propagate in a one-dimensional waveguide and interact with a two-level atom.

rise to non Markovian effects. In free space or in an open waveguide in which a spontaneously emitted photon cannot return again to the same atom such a recurrence contribution is impossible so that $T_1^{1,1}(t_2-t_1)$ and the term (1.17) both vanish. The same argument applies to all other diagrams of higher order. Thus, only the diagrams depicted in Figs. 1.5 (a) and 1.5 (b) contribute to the pure quantum state describing this process, i.e.

$$\begin{aligned} |\widetilde{\psi}(t)\rangle \;&=\; e^{-\frac{\Gamma}{2}(t-t_0)}\,|e\rangle_1\,|0\rangle^P \\ &\quad + \frac{\mathrm{i}}{\hbar}\,|g\rangle_1 \int_{t_0}^{t} \hat{\mathbf{E}}_\perp^-(\mathbf{x}_1,t_1)\cdot\mathbf{d}_1^*\,|0\rangle^P\, e^{-(\Gamma/2+\mathrm{i}\omega_{eg})(t_1-t_0)}dt_1\ . \end{aligned}$$

If many atoms are present the excitation of one atom can be transfered to another atom by the exchange of a photon which is emitted spontaneously by an excited atom and absorbed again later by an unexcited atom. In general such an excitation transfer from one atom to another mediated by the exchange of a single photon wave packet leads to non Markovian effects, especially if the distance between the two atoms is larger than the characteristic length c_0/Γ of the photon wave packet. A diagram describing such a process is depicted in Fig. 1.5 (d). This diagram describing the excitation transfer from atom 1 to atom 2 is associated with the term

$$-\,|e\rangle_2\,|0\rangle^P \int_{t_0}^{t}\int_{t_0}^{t_2} e^{-\Gamma(t-t_2)/2}T_1^{1,2}(t_2-t_1)e^{-\Gamma(t_1-t_0)/2}dt_1dt_2\ . \tag{1.18}$$

1.3.2
Scattering of two photons by a single atom

The photon path representation of Eq. (1.13) also describes saturation effects properly which come into play as soon as more than a single excitation is present in the atom-field system. In the following we investigate the scattering of two photons propagating in free space or in a waveguide by a single two-level atom at the fixed position $\mathbf{x}_1$. We assume that the atom is initially prepared in its ground state $|g\rangle_1$ and that two initial photonic excitations are present in the system. Thus, the initial state is given by

$$|\psi(t_0)\rangle = \left(\textstyle\sum_j f_j^{(2)}(t_0)a_j^\dagger\right)\left(\textstyle\sum_j f_j^{(1)}(t_0)a_j^\dagger\right)|0\rangle^P\,|g\rangle_1\ .$$

A corresponding sketch of a possible experimental setup using a one-dimensional waveguide is depicted in Fig. 1.6. The five diagrams contributing to the particular part of the quantum state $|\widetilde{\psi}(t)\rangle$ which describes two outgoing photons are depicted in Fig. 1.7. By adding up the associated terms we obtain the result

$$|\widetilde{\psi}^{\mathrm{out}}(t)\rangle = |\widetilde{\psi}^{(\mathrm{a})}(t)\rangle + |\widetilde{\psi}^{(\mathrm{b})}(t)\rangle + |\widetilde{\psi}^{(\mathrm{c})}(t)\rangle + |\widetilde{\psi}^{(\mathrm{d})}(t)\rangle + |\widetilde{\psi}^{(\mathrm{e})}(t)\rangle\ .$$

Thereby, the diagram depicted in Fig. 1.7 (a) corresponds to the term

$$|\widetilde{\psi}^{(\mathrm{a})}(t)\rangle = |\psi(t_0)\rangle = \left(\sum_j f_j^{(2)}(t_0)a_j^\dagger\right)\left(\sum_j f_j^{(1)}(t_0)a_j^\dagger\right)|0\rangle^P\,|g\rangle_1$$

and describes the unperturbed time evolution of both incoming photons. The diagrams in Figs. 1.7 (b) and 1.7 (c) describe scattering processes in which one of the two photons is absorbed by the atom at time t_1 and the atom emits the photon again spontaneously at the later time t_2. The other photon is propagating in an unperturbed way. These diagrams correspond to the terms

$$\begin{aligned}|\widetilde{\psi}^{(\mathrm{b})}(t)\rangle &= -\frac{1}{\hbar^2}\int_{t_0}^{t}\int_{t_0}^{t_2}\left(\hat{\mathbf{E}}_\perp^-(\mathbf{x}_1,t_2)\cdot\mathbf{d}_1^*\right)\left(\sum_j f_j^{(2)}(t_0)a_j^\dagger\right)\\ &\quad |0\rangle^P\,|g\rangle_1\,e^{-(\mathrm{i}\omega_{eg}+\Gamma/2)(t_2-t_1)}\left[\hat{\mathbf{E}}_\perp^+(\mathbf{x}_1,t_1)\cdot\mathbf{d}_1,\sum_j f_j^{(1)}(t_0)a_j^\dagger\right]dt_1dt_2\end{aligned}$$

and

$$\begin{aligned}|\widetilde{\psi}^{(\mathrm{c})}(t)\rangle &= -\frac{1}{\hbar^2}\int_{t_0}^{t}\int_{t_0}^{t_2}\left(\hat{\mathbf{E}}_\perp^-(\mathbf{x}_1,t_2)\cdot\mathbf{d}_1^*\right)\left(\sum_j f_j^{(1)}(t_0)a_j^\dagger\right)\\ &\quad |0\rangle^P\,|g\rangle_1\,e^{-(\mathrm{i}\omega_{eg}+\Gamma/2)(t_2-t_1)}\left[\hat{\mathbf{E}}_\perp^+(\mathbf{x}_1,t_1)\cdot\mathbf{d}_1,\sum_j f_j^{(2)}(t_0)a_j^\dagger\right]dt_1dt_2\,.\end{aligned}$$

The diagrams in Figs. 1.7 (d) and 1.7 (e) correspond to the terms

$$\begin{aligned}|\widetilde{\psi}^{(\mathrm{d})}(t)\rangle &= \frac{1}{\hbar^4}\int_{t_0}^{t}\int_{t_0}^{t_4}\int_{t_0}^{t_3}\int_{t_0}^{t_2}dt_1dt_2dt_3dt_4e^{-(\mathrm{i}\omega_{eg}+\Gamma/2)(t_2+t_4-t_1-t_3)}\\ &\quad \left(\hat{\mathbf{E}}_\perp^-(\mathbf{x}_1,t_4)\cdot\mathbf{d}_1^*\right)\left(\hat{\mathbf{E}}_\perp^-(\mathbf{x}_1,t_2)\cdot\mathbf{d}_1^*\right)|0\rangle^P\,|g\rangle_1\\ &\quad \left[\hat{\mathbf{E}}_\perp^+(\mathbf{x}_1,t_1)\cdot\mathbf{d}_1,\sum_j f_j^{(1)}(t_0)a_j^\dagger\right]\left[\hat{\mathbf{E}}_\perp^+(\mathbf{x}_1,t_3)\cdot\mathbf{d}_1,\sum_j f_j^{(2)}(t_0)a_j^\dagger\right]\end{aligned}$$

and

$$\begin{aligned}|\widetilde{\psi}^{(\mathrm{e})}(t)\rangle &= \frac{1}{\hbar^4}\int_{t_0}^{t}\int_{t_0}^{t_4}\int_{t_0}^{t_3}\int_{t_0}^{t_2}dt_1dt_2dt_3dt_4e^{-(\mathrm{i}\omega_{eg}+\Gamma/2)(t_2+t_4-t_1-t_3)}\\ &\quad \left(\hat{\mathbf{E}}_\perp^-(\mathbf{x}_1,t_4)\cdot\mathbf{d}_1^*\right)\left(\hat{\mathbf{E}}_\perp^-(\mathbf{x}_1,t_2)\cdot\mathbf{d}_1^*\right)|0\rangle^P\,|g\rangle_1\\ &\quad \left[\hat{\mathbf{E}}_\perp^+(\mathbf{x}_1,t_3)\cdot\mathbf{d}_1,\sum_j f_j^{(1)}(t_0)a_j^\dagger\right]\left[\hat{\mathbf{E}}_\perp^+(\mathbf{x}_1,t_1)\cdot\mathbf{d}_1,\sum_j f_j^{(2)}(t_0)a_j^\dagger\right].\end{aligned}$$

They describe scattering processes in which the atom absorbs and re-emits both of the photons one after the other. Thereby, the nonlinear features of these processes induced by saturation effects originates from the rule that the atom can only absorb a second photon after the first absorbed photon has already been re-emitted again.

1.3.3 Dynamics of two atoms

The photon path representation of Eq. (1.13) can also describe the dynamics of many atoms interacting with a radiation field or the non-Markovian retardation effects aris-

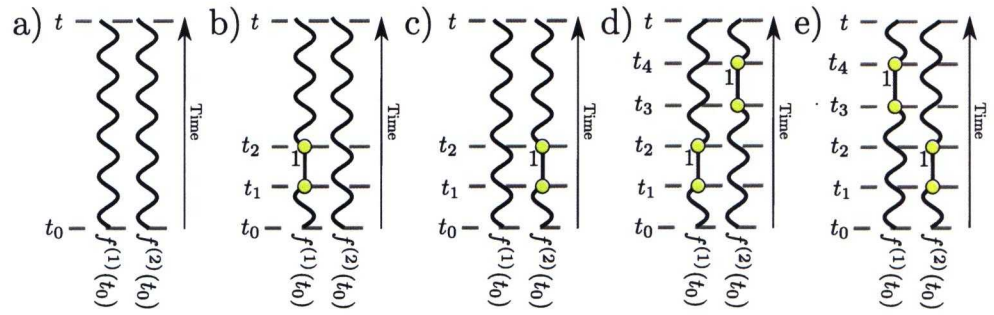

Figure 1.7 Diagrams describing the scattering of two photons by a single two-level atom.

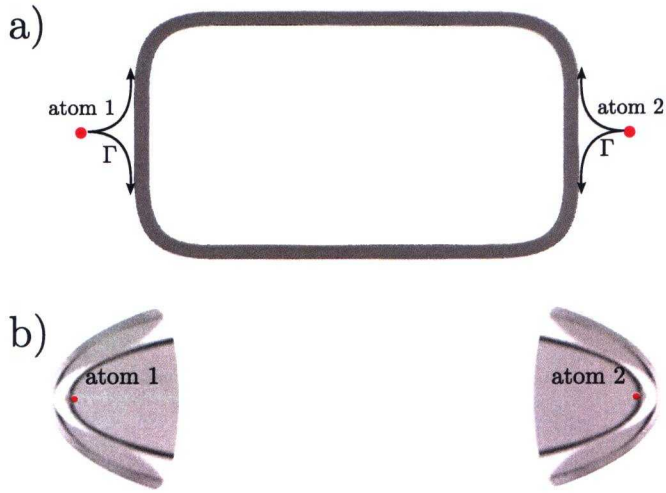

Figure 1.8 Two atoms coupled to a multimode radiation field: Photonic excitations can propagate from one atom to the other through a one-dimensional waveguide (a); photons are guided by two parabolic mirrors in free space (b). Both setups lead to the same atomic dynamics.

ing from the presence of a cavity. Such processes share the characteristic feature that a photon emitted by one atom can return again to the same atom at a later time or it may interact later with one of the residual atoms. In the following we investigate such a situation involving two two-level atoms as depicted schematically in Fig. 1.8 (a) for a waveguide or in Fig. 1.8 (b) for free-space scenario with two half open parabolic cavities. Both cases result in the same dynamics.

The setup depicted in Fig. 1.8 (a) consists of two atoms coupled to a common waveguide which forms a loop. Consequently, a photon emitted by one of the atoms can travel to the other atom or it can return again to the original atom. We assume that the atoms couple on to the modes of the radiation field which are guided by the one-dimensional waveguide. The corresponding free space setup is depicted in Fig. 1.8 (b). It consists of two parabolic mirrors facing each other and of two atoms. Each of these atoms is supposed to be trapped close to the focal points $\mathbf{x}_1$ and $\mathbf{x}_2$ of these parabolic mirrors. For the sake of simplicity we also assume that the dipole matrix elements of these atoms are oriented along the axis of symmetry of the setup. The

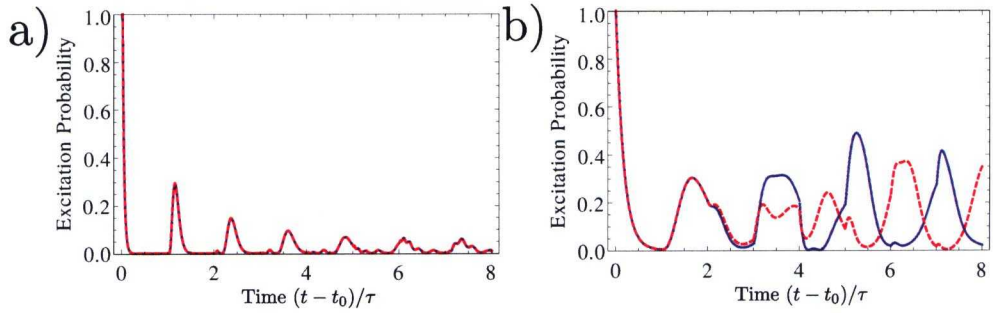

Figure 1.9 Time dependence of the probability of exciting both atoms: Exact solution obtained from the diagrammatic method (solid line), harmonic approximation replacing both two-level atoms by harmonic oscillators (dashed line). The parameters are $1 = \exp(\mathrm{i}2\tau\omega_{eg})$ with $\Gamma\tau = 15$ (a) and $\Gamma\tau = 3$ (b).

ideally conducting parabolic mirrors enhance the matter field interactions of the two atoms. In this case the exclusive coupling to the radiation field guided by the one-dimensional waveguide of Fig. 1.8 (a) corresponds to the limit that the mirrors cover almost the full solid angle around the atoms.

In the following we discuss the time evolution of the initial state $|\psi(t_0)\rangle = |e\rangle_1 |e\rangle_2 |0\rangle^P$ with the radiation field in its vacuum state and the two atoms being in their excited states. The waveguide as well as the free space scenario can be described by using the relations

$$\begin{aligned} \frac{1}{\hbar^2}\left[\hat{\mathbf{E}}_\perp^+(\mathbf{x}_1,t_2)\cdot\mathbf{d}_1, \hat{\mathbf{E}}_\perp^-(\mathbf{x}_1,t_1)\cdot\mathbf{d}_1^*\right] &= \frac{1}{\hbar^2}\left[\hat{\mathbf{E}}_\perp^+(\mathbf{x}_2,t_2)\cdot\mathbf{d}_2, \hat{\mathbf{E}}_\perp^-(\mathbf{x}_2,t_1)\cdot\mathbf{d}_2^*\right] \\ &= \Gamma\sum_{j\in\mathbb{Z}}\delta(t_2-t_1-2j\tau) \end{aligned} \tag{1.19}$$

and

$$\frac{1}{\hbar^2}\left[\hat{\mathbf{E}}_\perp^+(\mathbf{x}_1,t_2)\cdot\mathbf{d}_1, \hat{\mathbf{E}}_\perp^-(\mathbf{x}_2,t_1)\cdot\mathbf{d}_2^*\right] = \Gamma\sum_{j\in\mathbb{Z}}\delta(t_2-t_1-(2j+1)\,\tau)\,. \tag{1.20}$$

The constant τ denotes the typical time a photon needs to propagate from atom 1 to atom 2 [40]. With the help of the path representation and the relations of Eqs. (1.19) and (1.20), the time evolution of the matter-field system can be evaluated. A major difficulty is caused by the non-linear behavior originating from the saturation effects of the two excited atoms. However, by using the previously discussed diagrammatic method the probability of finding both atoms in their excited states at a later time can be determined in a straightforward way. The corresponding results are depicted in Figs. 1.9 (a) and 1.9 (b). It is worth comparing these results with the ones in which the non-linear behavior of the atoms is neglected. In such a harmonic approximation the two atoms can be replaced by harmonic oscillators according to the substitutions

$$|g\rangle_i\langle e|_i \to b_i,\ |e\rangle_i\langle g|_i \to b_i^\dagger,\ |e\rangle_i\langle e|_i \to b_i^\dagger b_i\ i\in\{1,2\} \tag{1.21}$$

with $b_i^\dagger$ and b_i denoting the creation and annihilation operators of a harmonic oscillator. In such a harmonic approximation the evaluation of the time evolution is simplified significantly because the Hamiltonian operator describes a system of coupled harmonic oscillators. Comparing the situations depicted in Figs. 1.9 (a) and 1.9 (b) one realizes that the harmonic approximation is appropriate in the case of Fig.

1.9 (a) but it fails completely in the case of Fig. 1.9 (b). This can be understood in a simple way because in the case of Fig. 1.9 (a) we have $\Gamma\tau \gg 1$ so that the probability, for example, that atom 2 is still excited before the photon emitted by atom 1 can reach it is very small. Consequently saturation effects are negligible. In the case of Fig. 1.9 (b) we have $\Gamma\tau$ so that this probability is no longer negligible. As a result saturation effects are significant.

1.4 Conclusion

We have developed a diagrammatic method suitable for investigating the time evolution of highly non-classical multiphoton number states interacting with multiple quantum emitters in extreme multimode scenarios. This method can be applied to study numerous cases of interest in quantum information processing, such as the dynamics of quantum emitters coupled to one-dimensional waveguides or to the radiation field in large or half-open cavities or even in free space. Thereby, each term of this photon path representation can be represented by a descriptive photon path involving sequences of spontaneous photon emission and absorption processes involving multiple atoms and multiple photons simultaneously. The accuracy of this diagrammatic method is only limited by the main standard quantum optical approximations, namely the dipole approximation and the assumption that the timescale induced by the atomic transition frequencies is by far the shortest one. Furthermore, it offers the unique feature that in order to obtain exact analytical expressions for a finite time interval only a finite number of diagrams has to be taken into account. By applying this diagrammatic method we are able to study the matter field interaction of single quantum emitters with highly non-classical multiphoton field states in scenarios ranging from free space or half-open cavities to waveguides. In particular, our method allows us to study nonlinear and non Markovian effects induced by matter field interactions on the single photon level. The investigation of these effects is not only interesting for possible applications in quantum information processing and quantum communication but also from the fundamental point of view. Thus, our method could be used to design suitable protocols for quantum information processing and quantum communication in a variety of architectures ranging from metallic nanowires coupled to quantum dots to possible applications in free space.

Appendix
Evaluation of the field commutator

In this section we evaluate the commutator

$$\begin{aligned} & e^{\mathrm{i}\omega_{eg}(t_2-t_1)}\left[\hat{\mathbf{E}}_{\perp}^{+}(\mathbf{x}_{A_2},t_2)\cdot\mathbf{d}_{A_2},\hat{\mathbf{E}}_{\perp}^{-}(\mathbf{x}_{A_1},t_1)\cdot\mathbf{d}_{A_1}^{*}\right] \\ &= \sum_i e^{\mathrm{i}(\omega_{eg}-\omega_i)(t_2-t_1)}\frac{\hbar\omega_i}{2\epsilon_0}\left(\mathbf{g}_i^{*}(\mathbf{x}_{A_2})\cdot\mathbf{d}_{A_2}\right)\left(\mathbf{g}_i(\mathbf{x}_{A_1})\cdot\mathbf{d}_{A_1}^{*}\right) \end{aligned} \tag{22}$$

which is identical to

$$e^{\mathrm{i}\omega_{eg}(t_2-t_1)}\left[\hat{\mathbf{E}}_{\perp}(\mathbf{x}_{A_2},t_2)\cdot\mathbf{d}_{A_2},\hat{\mathbf{E}}_{\perp}(\mathbf{x}_{A_1},t_1)\cdot\mathbf{d}_{A_1}^{*}\right]$$

apart from terms negligible under the assumption that the timescale induced by ω_{eg} is by far the shortest for the system's dynamics. Thus, in this approximation we conclude

$$\begin{aligned} & e^{\mathrm{i}\omega_{eg}(t_2-t_1)}\left[\hat{\mathbf{E}}_{\perp}^{+}(\mathbf{x}_{A_2},t_2)\cdot\mathbf{d}_{A_2},\hat{\mathbf{E}}_{\perp}^{-}(\mathbf{x}_{A_1},t_1)\cdot\mathbf{d}_{A_1}^{*}\right] \\ &= e^{\mathrm{i}\omega_{eg}(t_2-t_1)}\left[\hat{\mathbf{E}}_{\perp}(\mathbf{x}_{A_2},t_2)\cdot\mathbf{d}_{A_2},\hat{\mathbf{E}}_{\perp}(\mathbf{x}_{A_1},t_1)\cdot\mathbf{d}_{A_1}^{*}\right]. \end{aligned} \tag{23}$$

Furthermore, we have the relation

$$\begin{aligned} & \left[\hat{\mathbf{E}}_{\perp}(\mathbf{x}_{A_2},t_2)\cdot\mathbf{d}_{A_2},\hat{\mathbf{E}}_{\perp}(\mathbf{x}_{A_1},t_1)\cdot\mathbf{d}_{A_1}^{*}\right] \\ &= -\tfrac{\mathrm{i}\hbar}{\epsilon_0}\mathbf{d}_{A_2}\cdot\nabla\times\nabla\times\left[\mathbf{G}(\mathbf{x}_{A_2},\mathbf{x}_{A_1},t_2-t_1)-\mathbf{G}(\mathbf{x}_{A_2},\mathbf{x}_{A_1},t_1-t_2)\right]\cdot\mathbf{d}_{A_1}^{*} \end{aligned} \tag{24}$$

with $\mathbf{G}(\mathbf{x},\mathbf{x}',t)$ denoting the dyadic Green operator of the electromagnetic radiation field. It satisfies the defining equation

$$\Box\mathbf{G}(\mathbf{x},\mathbf{x}',t)=\delta_{\perp}^{3}(\mathbf{x}-\mathbf{x}')\delta(t)\ ,\mathbf{G}(\mathbf{x},\mathbf{x}',t)=0\ \forall t<0 \tag{25}$$

with $\delta_{\perp}^{3}$ denoting the transversal delta distribution. This equation has to be solved under the boundary conditions modelling a possible cavity. Combining Eqs. (23) and (24) we obtain the relation

$$\begin{aligned} & \left[\hat{\mathbf{E}}_{\perp}^{+}(\mathbf{x}_{A_2},t_2)\cdot\mathbf{d}_{A_2},\hat{\mathbf{E}}_{\perp}^{-}(\mathbf{x}_{A_1},t_1)\cdot\mathbf{d}_{A_1}^{*}\right] \\ &= -\tfrac{\mathrm{i}\hbar}{\epsilon_0}\mathbf{d}_{A_2}\cdot\left[\nabla\times\nabla\times\mathbf{G}(\mathbf{x}_{A_2},\mathbf{x}_{A_1},t_2-t_1)-\nabla\times\nabla\times\mathbf{G}(\mathbf{x}_{A_2},\mathbf{x}_{A_1},t_1-t_2)\right]\mathbf{d}_{A_1}^{*}. \end{aligned}$$

Due to the finite speed of light in vacuum c_0 the dyadic Green operator $\mathbf{G}(\mathbf{x},\mathbf{x}',t)$ exhibits retardation effects. These retardation effects are inherited by the commutator $\left[\hat{\mathbf{E}}_{\perp}^{+}(\mathbf{x}_{A_2},t_2)\cdot\mathbf{d}_{A_2},\hat{\mathbf{E}}_{\perp}^{-}(\mathbf{x}_{A_1},t_1)\cdot\mathbf{d}_{A_1}^{*}\right]$ and lead to the properties described in Eq. (1.10). Eq. (1.10) can be derived by using the well known expression for the dyadic Green operator $\mathbf{G}(\mathbf{x},\mathbf{x}',t)$ in free space. In fact, Eq. (1.10) contains an additional purely imaginary term which reflects a level shift (Lamb-shift) and which can be incorporated into a properly renormalized atomic transition frequency ω_{eg}.

References

1 Berman, P. (ed.) (1994) *Cavity Quantum Electrodynamics*, Academic Press, San Diego.

2 Walther, H., Varcoe, B.T., Englert, B.G., and Becker, T. (2006) Cavity quantum electrodynamics. *Prog. Phys.*, **69**, 1325.

3 Haroche, S. and Raimond, J.M. (2006) *Exploring the Quantum: Atoms, Cavities and Photons*, Oxford University Press, Oxford.

4 Goy, P., Raimond, J., Gross, M., and Haroche, S. (1983) Observation of cavity-enhanced single-atom spontaneous emission. *Phys. Rev. Lett.*, **50**, 1903–1906.

5 Meschede, D., Walther, H., and Müller, G. (1985) One-atom maser. *Phys. Rev. Lett.*, **54** (6), 551.

6 McKeever, J., Boca, A., Boozer, A.D., Buck, J.R., and Kimble, H.J. (2003) Experimental realization of a one-atom laser in the regime of strong coupling. *Nature*, **425**, 268–271.

7 Reiserer, A., Ritter, S., and Rempe, G. (2013) Nondestructive detection of an optical photon. *Science*, **342** (6164), 1349–1351.

8 Reiserer, A., Kalb, N., Rempe, G., and Ritter, S. (2014) A quantum gate between a flying optical photon and a single trapped atom. *Nature*, **508** (7495), 237–240.

9 Kalb, N., Reiserer, A., Ritter, S., and Rempe, G. (2015) Heralded storage of a photonic quantum bit in a single atom. *Phys. Rev. Lett.*, **114**, 220 501.

10 Boozer, A.D., Boca, A., Miller, R., Northup, T.E., and Kimble, H.J. (2007) Reversible state transfer between light and a single trapped atom. *Phys. Rev. Lett.*, **98** (19), 193 601.

11 Hofheinz, M., Wang, H., Ansmann, M., Bialczak, R.C., Lucero, E., Neeley, M., O'Connell, A., Sank, D., Wenner, J., Martinis, J.M. *et al.* (2009) Synthesizing arbitrary quantum states in a superconducting resonator. *Nature*, **459** (7246), 546–549.

12 Chang, D., Sørensen, A.S., Hemmer, P., and Lukin, M. (2006) Quantum optics with surface plasmons. *Phys. Rev. Lett.*, **97** (5), 053 002.

13 Akimov, A., Mukherjee, A., Yu, C., Chang, D., Zibrov, A., Hemmer, P., Park, H., and Lukin, M. (2007) Generation of single optical plasmons in metallic nanowires coupled to quantum dots. *Nature*, **450** (7168), 402–406.

14 Schuller, J.A., Barnard, E.S., Cai, W., Jun, Y.C., White, J.S., and Brongersma, M.L. (2010) Plasmonics for extreme light concentration and manipulation. *Nature materials*, **9** (3), 193–204.

15 Babinec, T.M., Hausmann, B.J., Khan, M., Zhang, Y., Maze, J.R., Hemmer, P.R., and Lončar, M. (2010) A diamond nanowire single-photon source. *Nature nanotechnology*, **5** (3), 195–199.

16 Claudon, J., Bleuse, J., Malik, N.S., Bazin, M., Jaffrennou, P., Gregersen, N., Sauvan, C., Lalanne, P., and Gérard, J.M. (2010) A highly efficient single-photon source based on a quantum dot in a photonic nanowire. *Nature Photonics*, **4** (3), 174–177.

17 Vetsch, E., Reitz, D., Sagué, G., Schmidt, R., Dawkins, S., and Rauschenbeutel, A. (2010) Optical interface created by laser-cooled atoms trapped in the evanescent field surrounding an optical nanofiber. *Phys. Revi. Lett.*, **104** (20),

203 603.

18 Goban, A., Choi, K.S., Alton, D.J., Ding, D., Lacroûte, C., Pototschnig, M., Thiele, T., Stern, N.P., and Kimble, H.J. (2012) Demonstration of a state-insensitive, compensated nanofiber trap. *Phys. Rev. Lett.*, **109**, 033 603.

19 You, J. and Nori, F. (2011) Atomic physics and quantum optics using superconducting circuits. *Nature*, **474** (7353), 589–597.

20 Devoret, M. and Schoelkopf, R. (2013) Superconducting circuits for quantum information: an outlook. *Science*, **339** (6124), 1169–1174.

21 Maiwald, R., Golla, A., Fischer, M., Bader, M., Heugel, S., Chalopin, B., Sondermann, M., and Leuchs, G. (2012) Collecting more than half the fluorescence photons from a single ion. *Phys.Rev.A*, **86** (4), 043 431.

22 Varcoe, B.T., Brattke, S., Weidinger, M., and Walther, H. (2000) Preparing pure photon number states of the radiation field. *Nature*, **403** (6771), 743–746.

23 Hofheinz, M., Weig, E., Ansmann, M., Bialczak, R.C., Lucero, E., Neeley, M., Oconnell, A., Wang, H., Martinis, J.M., and Cleland, A. (2008) Generation of fock states in a superconducting quantum circuit. *Nature*, **454** (7202), 310–314.

24 Waks, E., Diamanti, E., and Yamamoto, Y. (2006) Generation of photon number states. *New Journal of Physics*, **8** (1), 4.

25 Bethe, H. (1931) Zur theorie der metalle. *Z. Phys.*, **71** (3-4), 205–226.

26 Gardiner, C.W. and Collett, M.J. (1985) Input and output in damped quantum systems: Quantum stochastic differential equations and the master equation. *Phys. Rev. A*, **31**, 3761–3774.

27 Shen, J.T. and Fan, S. (2007) Strongly correlated two-photon transport in a one-dimensional waveguide coupled to a two-level system. *Phys. Rev. Lett.*, **98**, 153 003.

28 Fan, S., Kocabaş, Ş.E., and Shen, J.T. (2010) Input-output formalism for few-photon transport in one-dimensional nanophotonic waveguides coupled to a qubit. *Phys.Rev.A*, **82** (6), 063 821.

29 Shi, T. and Sun, C.P. (2009) Lehmann-symanzik-zimmermann reduction approach to multiphoton scattering in coupled-resonator arrays. *Phys. Rev. B*, **79**, 205 111.

30 Zheng, H., Gauthier, D.J., and Baranger, H.U. (2010) Waveguide qed: Many-body bound-state effects in coherent and fock-state scattering from a two-level system. *Phys.Rev.A*, **82** (6), 063 816.

31 Roy, D. (2011) Two-photon scattering by a driven three-level emitter in a one-dimensional waveguide and electromagnetically induced transparency. *Phys. Rev. Lett.*, **106**, 053 601.

32 Xu, S. and Fan, S. (2015) Input-output formalism for few-photon transport: A systematic treatment beyond two photons. *Phys. Rev. A*, **91**, 043 845.

33 Caneva, T., Manzoni, M.T., Shi, T., Douglas, J.S., Cirac, J.I., and Chang, D.E. (2015) Quantum dynamics of propagating photons with strong interactions: a generalized input-output formalism. *arXiv preprint arXiv:1501.04427*.

34 Shi, T., Chang, D.E., and Cirac, J.I. (2015) Multiphoton-scattering theory and generalized master equations. *Phys. Rev. A*, **92**, 053 834.

35 Mollow, B. (1975) Pure-state analysis of resonant light scattering: Radiative damping, saturation, and multiphoton effects. *Phys.Rev.A*, **12** (5), 1919.

36 Weisskopf, V.F. and Wigner, E.P. (1930) Calculation of the natural brightness of spectral lines on the basis of dirac's theory. *Z. Phys.*, **63**, 54–73.

37 Alber, G., Bernád, J.Z., Stobińska, M., Sánchez-Soto, L.L., and Leuchs, G. (2013) Qed with a parabolic mirror. *Phys. Rev. A*, **88**, 023 825.

38 Alber, G. (1992) Photon wave packets and spontaneous decay in a cavity. *Phy. Rev. A*, **46** (R5338), R5338.

39 Milonni, P.W. and Knight, P.L. (1974) Retardation in the resonant interaction of two identical atoms. *Phy. Rev. A*, **10**, 1096–1108.

40 Trautmann, N., Bernád, J.Z., Sondermann, M., Alber, G., Sánchez-Soto, L.L., and Leuchs, G. (2014) Generation of entangled matter qubits in two opposing parabolic mirrors. *Phys.Rev.A*, **90**, 063 814.